JOURNAL OF PHYSICAL ORGANIC CHEMISTRY
J. Phys. Org. Chem. 2000: **13;** 23–34

^{15}N NMR study of proton localization and proton transfer thermodynamics and kinetics in polycrystalline porphycene†

Uwe Langer,[1] Christof Hoelger,[1]‡ Bernd Wehrle,[1]§ Lidia Latanowicz,[2] Emanuel Vogel[3] and Hans-Heinrich Limbach[1]*

[1]Fachbereich Biologie, Chemie, Pharmazie, Freie Universität Berlin, Takustrasse 3, D-14195 Berlin, Germany
[2]Institute of Physics, Pedagogical University, Plac Slowianski 6, 65-069 Zielona Gora, Poland
[3]Institut für Organische Chemie der Universität Köln, Greinstr.4, D-50939 Cologne, Germany

Received 20 January 1999; revised 18 August 1999; accepted 23 August 1999

ABSTRACT: Using high-resolution solid-state ^{15}N cross-polarization magic angle spinning NMR techniques, the proton transfer thermodynamics and dynamics and the proton locations in polycrystalline ^{15}N-labeled porphycene were studied. Whereas at room temperature only a single ^{15}N resonance is observed, indicating an equivalence of all nitrogen atoms arising from a quasi-degenerate fast proton transfer, four signals are observed at low temperatures, exhibiting temperature-dependent line positions. Their analysis is consistent with the presence of either (i) two different molecules A and B in the asymmetric unit, each of which is subject to a quasi-degenerate correlated double proton transfer, or (ii) a single molecule exhibiting all four possible near-degenerate tautomeric states, two *trans*- and two *cis*-tautomers, interconverting by fast single proton transfers. The average rate constants of the proton transfer processes are found to be in the nanosecond time-scale. These constants were obtained between 228 and 355K by analysis of the longitudinal 9.12 MHz ^{15}N T_1 relaxation times, which exhibit a minimum around 280 K. The relaxation analysis was performed in terms of a quasi-degenerate two-state proton transfer process which modulates the heteronuclear ^{1}H–^{15}N dipole–dipole interaction. From the value of T_1 in the minimum, the crystallographic NN distance of 2.63 Å and the hydrogen bond correlation for N—H···N hydrogen bonded systems, the two N···H distances of 1.10 and 1.60 Å were obtained, i.e. a hydrogen bond angle of 152°, which are significantly different from the corresponding values of 1.03 and 2.28 Å and 116° found for porphyrin. The analysis of the temperature dependence of the rate constants indicates tunneling as a major reaction pathway, involving a barrier of about 32 kJ mol^{-1}. The finding of a larger NH distance and a smaller barrier for proton transfer as compared with porphyrin is rationalized in terms of the stronger intramolecular hydrogen bonds in porphycene. A strong coupling between these bonds would indicate that the proton tautomerism in porphycene corresponds to a correlated double proton transfer, in contrast to the stepwise transfer in porphyrin. Finally, a relation between the intrinsic ^{15}N chemical shifts of porphyrinoids and the N···H distance was found, which might be useful for estimating geometries of porphyrinoids. Copyright © 2000 John Wiley & Sons, Ltd.

KEYWORDS: polycrystalline porphycene; proton localization; proton transfer; thermodynamics; kinetics; ^{15}N NMR

INTRODUCTION

The proton tautomerism of heterocyclic compounds is a topic of continuing interest because of its intimate relation with the problem of the structure of this class of compounds.[1] One challenge in this area of research is to design molecules exhibiting hydrogen-bonded structures in the solid state in such a way that one or more protons can be transferred either between different molecules such as pyrazoles[2] or inside molecules such as porphyrins[3] or tetraazaannulenes.[4] The barriers for proton transfer depend strongly on the molecular structure and the strength of the hydrogen bonds. Therefore, these molecules serve as reaction models to test various proton transfer theories and also theories of kinetic isotope effects.[2,3]

In the electronic ground states, degenerate or near-degenerate tautomeric processes of heterocycles are preferentially studied by NMR spectroscopy. As most proton transfers of heterocyclic compounds occur to and from nitrogen, ^{15}N NMR is especially suited to study these reactions; because of the spin 1/2 of ^{15}N, problems

**Correspondence to:* H.-H. Limbach, Fachbereich Biologie, Chemie, Pharmazie, Freie Universität Berlin, Takustrasse 3, D-14195 Berlin, Germany.
†Dedicated to Professor J. Elguero on the occasion of his 65th birthday.
‡Present address: Beiersdorf AG, Offenburg, Germany.
§Present address: Bayer AG, Leverkusen, Germany.
Contract/grant sponsor: Deutsche Forschungsgemeinschaft.
Contract/grant sponsor: Fonds der Chemischen Industrie.

 CCC 0894–3230/2000/010023–12 $17.50

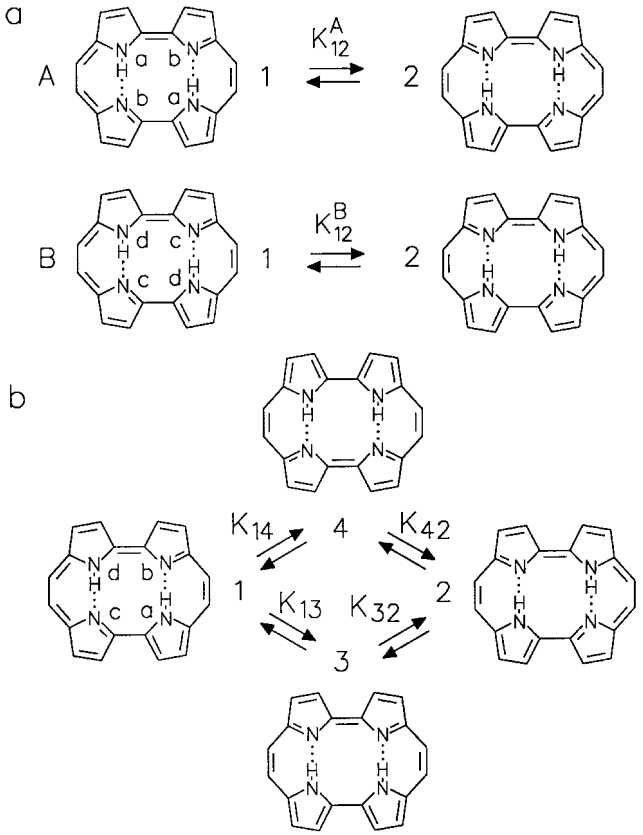

Figure 1. Tautomerism of porphycene in the crystalline state according to Ref. 3b. (a) Exchange model involving two non-degenerate correlated double proton transfers in two different molecules A and B in the asymmetric unit, each characterized by slightly different equilibrium constants K_{12}^{A} and K_{12}^{B}. (b) Exchange model involving single proton transfers between four tautomeric states 1–4

associated with the quadrupole moment of ^{14}N are avoided.[2,3] Therefore, some of us have exploited in recent years the use of solid-state ^{15}N NMR under the conditions of cross-polarization (CP), proton decoupling and magic angle spinning (MAS) in order to characterize the tautomerism of solid heterocycles.[2–6] Generally, the compounds have to be labeled with ^{15}N in order to obtain dynamic information concerning the proton transfer processes. Thus, it has been possible to determine protonation sites and equilibrium constants of proton transfer in solid ^{15}N-enriched heterocyclic compounds in a wide temperature range. In addition, rate constants could be obtained on the second time-scale by magnetization transfer techniques[2q,5] and on the millisecond time-scale using lineshape analysis.[2–4] Faster processes in systems with stronger hydrogen bonds could not be detected until recently when it was shown that the dipolar ^{1}H–^{15}N interaction is modulated by the proton tautomerism. A detailed analysis of the longitudinal ^{15}N relaxation times of the polycrystalline powder of several heterocycles showed that the rate constants of proton transfer could be obtained on the micro- to nanosecond time-scale.[2s,6]

In this paper, we report a study of the thermodynamics and the nanosecond time-scale proton transfer kinetics in polycrystalline porphycene (Fig. 1). This molecule exhibits two short intramolecular N—H···N hydrogen bonds in the crystalline state, as demonstrated by room-temperature x-ray crystallography[7] (Fig. 2). The asymmetric unit consists of only half a molecule because the molecule is located on an inversion center. A second molecule in the unit cell is related to the first one by symmetry. These findings imply that the two imino hydrogens are statistically disordered at room temperature. In a ^{15}N CP/MAS NMR study of the polycrystalline material, evidence was obtained that the protons in this compound are subject to a rapid degenerate tautomerism[3b] which confirms the room-temperature x-ray structure. However, at lower temperatures a splitting into four signals was observed which is consistent with either of the reaction schemes in Fig. 1. In Fig. 1(a) there are two slightly different molecules, A and B, in the crystal exhibiting a double proton transfer between two states 1 and 2. These states probably correspond to the tautomers with a diagonal arrangement of the protons. In contrast to the gas phase, the two states differ slightly in energy because of perturbations arising from the crystal field. We shall call this mechanism the 'correlated' double proton transfer mechanism according to a definition of Rumpel and Limbach[8] as no intermediate involving a vicinal arrangement of the two protons is directly observable. The actual transfer could still be

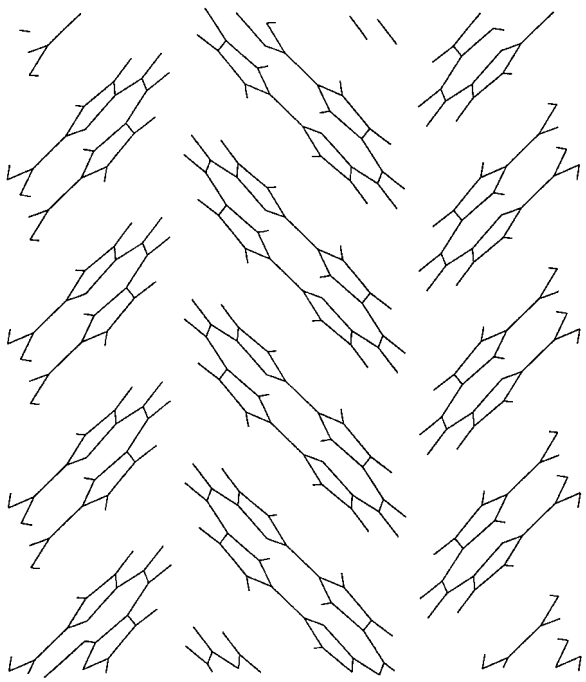

Figure 2. Crystal structure of porphycene according to Ref. 7

stepwise or concerted. The mechanism in Fig. 1(b) consists of single proton transfers between all possible four tautomeric states 1–4. In the following we shall call this mechanism the 'stepwise' mechanism as it clearly involves metastable intermediates with the protons in a vicinal arrangement.

Since the discovery of the proton tautomerism of porphycene,[3b] the hydrogen bond dynamics of this compound in the electronic ground state and the excited state have been of special interest.[9] For porphycene embedded in a matrix, a splitting in the electronic spectra was observed associated with a coherent tunnel splitting.[10] Recently, it was shown that alkyl-substituted porphycenes exhibit a similar solid-state tautomerism to the parent compound.[3g] However, so far it has not been possible to determine rate constants of the proton tautomerism of porphycenes. Such constants which are found to be on the nanosecond time-scale will be reported in this paper using longitudinal ^{15}N relaxometry.

This paper is organized as follows. In the Experimental section we describe briefly the methods and procedures used in this study. We then present the results of a variable-temperature ^{15}N chemical shift analysis by which the thermodynamic parameters of the two exchange mechanisms in Fig. 1 are established. Unfortunately, this analysis does not allow us to distinguish between the correlated and the stepwise transfer mechanisms. Subsequently the $^{15}NT_1$ relaxation times are reported and analyzed. From this analysis information about the hydrogen bond geometries, in particular the proton locations, and about the rate constants of proton transfer in porphycene is derived. The kinetic results are discussed in terms of a modified Bell tunneling model[3d,3f,11] in comparison with the isomer porphyrin and its anion studied previously. Finally, the nature of the proton tautomerism in porphycene is discussed.

EXPERIMENTAL

The synthesis of ^{15}N-enriched porphycene has been described previously.[3b] The $^{15}NT_1$ relaxation times of porphycene were measured between 203 and 341 K using a Bruker CXP 100 NMR spectrometer at 2.1 T, corresponding to a Larmor frequency of 9.12 MHz under ^{15}N CP/MAS conditions. For this purpose, the usual pulse sequence described by Torchia[12] without proton decoupling during the equilibration period of time was employed. In order to suppress artifacts arising from a distorted baseline and from acoustic ringing, the scheme of Du Bois Murphy[13] was employed. The 90° pulse width was 6 μs for both ^{1}H and ^{15}N. Cross-polarization times were around 6 ms. A spinning frequency of 2 kHz was sufficient to obtain spectra free from rotational sidebands. All chemical shifts are referenced to solid $^{15}NH_4Cl$.[14,15]

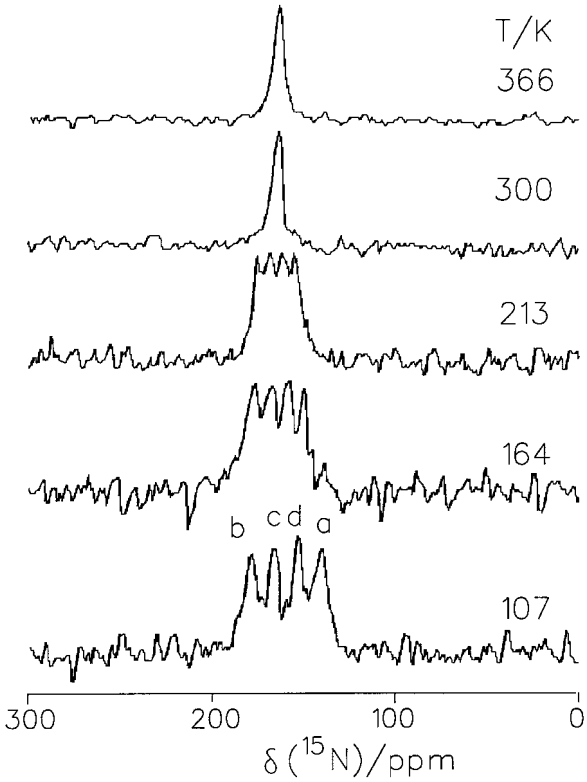

Figure 3. ^{15}N CP/MAS NMR spectra of 95% ^{15}N-enriched polycrystalline porphycene at 9.12 MHz as a function of temperature. 6 ms CP time, 5 kHz spectral width, 2.7s repetition time. Reference: external $^{15}NH_4Cl$. Average number of scans: 1200. Adapted from Ref. 3b

RESULTS

Variable-temperature ^{15}N CP/MAS NMR spectra of porphycene and thermodynamics of the solid-state proton tautomerism

In Figure 3 are assembled the ^{15}N CP/MAS NMR spectra of porphycene which have been described previously.[3b] At high temperature a single line is observed at 161 ppm (reference solid $^{15}NH_4Cl$), which indicates that all four nitrogen atoms are equivalent. However, as the temperature is lowered the signal splits into four sharp lines characterized by the chemical shifts δ_a, δ_b, δ_c and δ_d. The splittings $\delta_{ba} = \delta_b - \delta_a$ and $\delta_{cd} = \delta_c - \delta_d$ increase slightly with decreasing temperature and are listed in Table 1. These findings were explained[3b] by the presence of two non-equivalent, slightly asymmetric proton transfer systems:

$$N_m\text{—}H\cdots N_n \rightleftharpoons N_m\cdots H\text{—}N_n,\ mn = \text{ab, dc}$$

in which the protons move in slightly asymmetric double minimum potentials, and which are characterized by

Table 1. ^{15}N chemical shift differences of polycrystalline porphycene

T (K)	δ_{ba} (ppm)	δ_{cd} (ppm)
107	37.81	13.93
164	27.86	9.95
213	19.9	5.97
300	2*	2*
366	2*	2*

*estimated values.

different proton density ratios given by[4e]

$$K_{ab} = (1 - \delta_{ba}/\Delta)/(1 + \delta_{ba}/\Delta),$$
$$K_{dc} = (1 - \delta_{cd}/\Delta)/(1 + \delta_{cd}/\Delta) \quad (1a)$$

i.e.

$$\delta_{ba} = \Delta(1 - K_{ab})/(1 + K_{ab}),$$
$$\delta_{cd} = \Delta(1 - K_{dc})/(1 + K_{dc}) \quad (1b)$$

$\Delta = \delta_N - \delta_{NH}$ is the intrinsic chemical shift difference between the protonated and the non-protonated nitrogen atoms of porphycene. is assumed to be independent of temperature.

As pointed out in Ref. 3b, the findings in Fig. 3 can be explained in terms of the correlated proton transfer mechanisms or in terms of the stepwise mechanism illustrated in Fig. 1. The first assumes the presence of two different porphycene molecules A and B in the unit cell, where A contains two equivalent proton transfer units of the type N_a—H$\cdots$$N_b$ and B two equivalent units of the type N_d—H$\cdots$$N_c$. In this case the relations

$$K_{ab} = {K_{12}}^{A} = {x_2}^{A}/{x_1}^{A} = {a_{12}}^{A}\exp(-{b_{12}}^{A}/T),$$
$${a_{12}}^{A} = \exp(\Delta {S_{12}}^{A}/R), {b_{ij}}^{A} = \Delta {H_{ij}}^{A}/R \quad (2a)$$

$$K_{dc} = {K_{12}}^{B} = {x_2}^{B}/{x_1}^{B} = {a_{12}}^{B}\exp(-{b_{12}}^{B}/T),$$
$${a_{12}}^{B} = \exp(\Delta {S_{12}}^{B}/R), {b_{ij}}^{B} = \Delta {H_{ij}}^{B}/R \quad (2b)$$

are valid, where ${K_{12}}^{A}$ and ${K_{12}}^{B}$ represent the true equilibrium constants of the tautomeric processes in molecules A and B, $\Delta {S_{12}}^{A}$, $\Delta {S_{12}}^{B}$, $\Delta {H_{12}}^{A}$ and $\Delta {H_{12}}^{B}$ are the corresponding reaction entropies and enthalpies, R the gas constant and T the absolute temperature. The degeneracy between the two states is lifted by the crystal lattice—a very common situation in the tautomerism of solid heterocycles[3,4]—where the perturbation is larger for molecule A than for molecule B.

In the case of the stepwise transfer mechanism in Fig. 1(b), each porphycene molecule incorporates both proton transfer systems N_a—H$\cdots$$N_b$ and N_d—H$\cdots$$N_c$. This situation has also been found in the case of tetramethyldibenzotetraaza[14]annulene (TTAA), as proved using two-dimensional solid-state ^{15}N NMR.[4b–e] As the degeneracy between the two *trans*- and the two *cis*-tautomers is lifted by the crystal lattice, the average temperature-dependent proton densities are different at each nitrogen nucleus, giving rise to four different averaged lines in Fig. 3 at low temperatures.

The thermodynamics of the reaction network in Fig. 1(b) can be obtained in a similar way as in TTAA,[4d] as shown in the following. The proton density ratios are related to the equilibrium constants of the reaction network in Fig. 1(b) by

$$K_{ab} = (x_2 + x_4)/(x_1 + x_3)$$
$$= (K_{12} + K_{14})/(1 + K_{13}) \quad (3)$$

and

$$K_{dc} = (x_2 + x_3)/(x_1 + x_4)$$
$$= (K_{12} + K_{13})/(1 + K_{14}) \quad (4)$$

where

$$K_{ij} = x_j/x_i = a_{ij}\exp(-b_{ij}/T), a_{ij}$$
$$= \exp(\Delta S_{ij}/R), b_{ij} = \Delta H_{ij}/R \quad (5)$$

x_i is the mole fractions of the tautomeric state i and ΔS_{ij} and ΔH_{ij} are the reaction entropy and reaction

Table 2. Parameters of the van't Hoff analysis of Fig. 4[a]

Δ	${a_{12}}^{A}$	${b_{12}}^{A}$	${a_{12}}^{B}$	${b_{12}}^{B}$	$\Delta {S_{12}}^{A}$	ΔH_{12}^{A}	ΔS_{12}^{B}	ΔH_{12}^{B}
46	2.2	350	1.2	85	6.6	2.9	1.5	0.71

[a] Intrinsic chemical shift difference Δ in ppm, reaction enthalpies ΔH_{ij} in kJ mol^{-1} and reaction entropies ΔS_{ij} in J K^{-1} mol^{-1}.

Table 3. Parameters of the van't Hoff analysis of Fig. 5[a]

Δ	a_{12}	b_{12}	a_{13}	b_{13}	a_{14}	b_{14}	ΔS_{12}	ΔH_{12}	ΔS_{13}	ΔH_{13}	ΔS_{14}	ΔH_{14}
52	2	327	1.1	78	2	316	5.8	2.7	0	0.67	5.8	2.7

[a] Intrinsic chemical shift difference Δ in ppm, reaction enthalpies ΔH_{ij} in kJ mol^{-1} and reaction entropies ΔS_{ij} in J K^{-1} mol^{-1}.

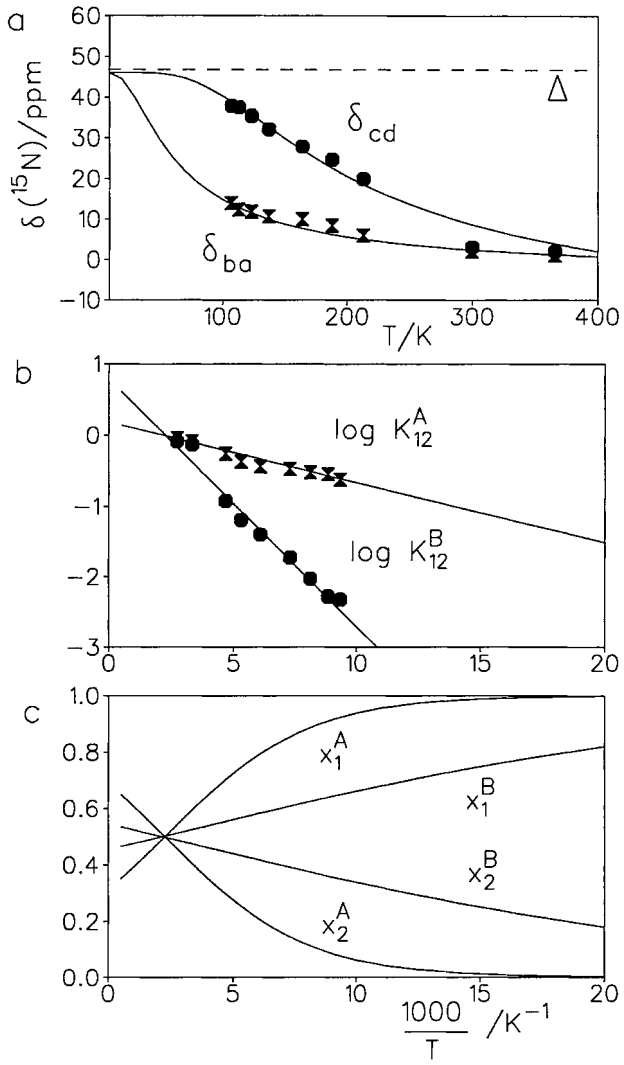

Figure 4. Thermodynamics of the porphycene tautomerism according to the exchange model in Fig. 1(a) (a) Comparison of the experimental temperature-dependent chemical shift separations δ_{ba} and δ_{cd} defined in Eqn. (1) with the theoretical values calculated as described in the text. Δ is the intrinsic chemical shift difference between non-protonated and protonated porphycene nitrogen atoms. (b) Van't Hoff diagram of $K_{12}{}^{A}$ and log $K_{12}{}^{B}$ as a function of the inverse temperature. (c) Calculated populations of tautomers 1 and 2 in molecules A and B as a function of the inverse temperature

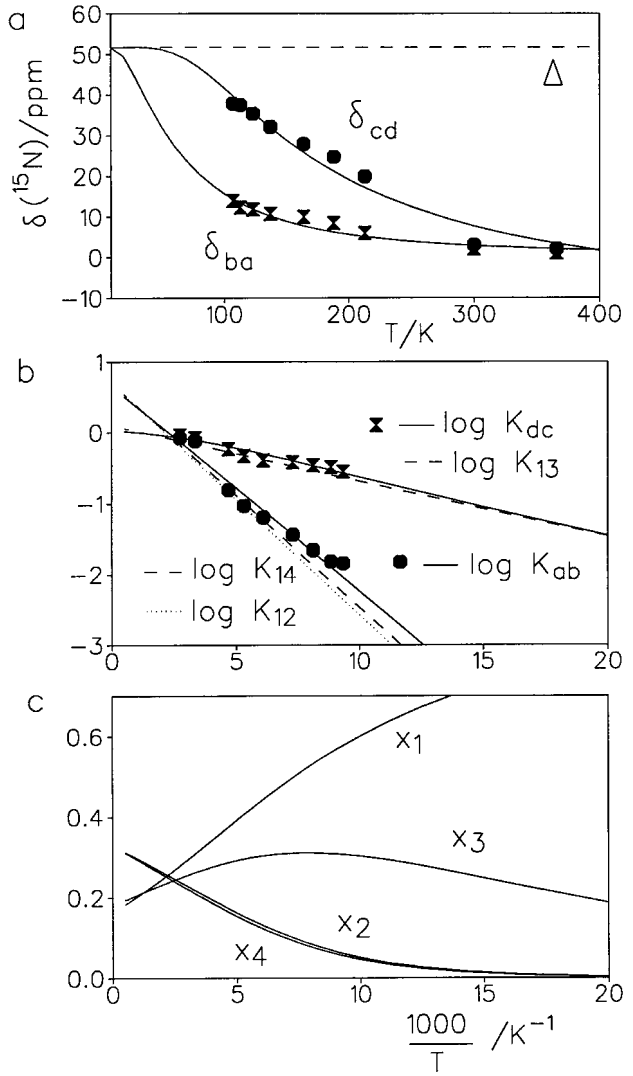

Figure 5. Thermodynamics of the porphycene tautomerism according to the exchange model in Fig. 1(a) (a) Comparison of the experimental temperature-dependent chemical shift separations δ_{ba} and δ_{cd} defined in Eqn. (1) with the theoretical values. (b) Van't Hoff diagram of the proton density ratios K_{ab} and K_{dc} defined in Eqns (3) and (4). (c) Calculated populations of tautomers 1–4 in Fig. 1 as a function of the inverse of temperature

enthalpy of the reaction step *ij*. By combination of Eqns (3)–(5) it follows that

$$\ln K_{ab} = \ln[a_{12}\exp(-b_{12}/T) + a_{14}\exp(-b_{14}/T)] - \ln[1 + a_{13}\exp(-b_{13}/T)] \quad (6)$$

and

$$\ln K_{ab} = \ln[a_{12}\exp(-b_{12}/T) + a_{13}\exp(-b_{13}/T)] - \ln[1 + a_{14}\exp(-b_{14}/T)] \quad (7)$$

In order to calculate K_{ab} and K_{dc} from the observed splittings δ_{ba} and δ_{cd}, the intrinsic chemical shift difference Δ must be known. In the case of porphyrin a value of Δ ppm = 108 was found in the slow proton exchange regime at low temperatures.[3b] In the case of porphycene, proton transfer is too fast and the deviations of the equilibrium constants from unity not large enough in order to determine the value of Δ at low temperatures in the 100 K region where liquid nitrogen can be used as a cooling gas. As pointed out in Ref. 3b, the use of the porphyrin value for the determination of equilibrium constants of the proton tautomerism of porphycene, a procedure employed in Ref. 3g, is only a crude

Table 4. ^{15}N T_1 relaxation times of polycrystalline porphycene obtained under MAS conditions

9.12 MHz						30.41 MHz		
T(K)	T_1(s)	σ	T(K)	T_1(s)	σ	T(K)	T_1(s)	σ
228	3.4	0.25	289	0.99	0.08	261	3	0.24
243	1.43	0.4	300	1.07	0.08	273	2.14	0.13
243.5	1.5	70.2	325	1.28	0.15	283	2.23	0.26
258	1.04	0.04	340	1.62	0.13	284	2.3	0.13
269	0.97	0.03	355	2.7	0.27	292	2.35	0.14
279	0.98	0.99	—	—	—	305	1.66	0.12

approximation which leads to erroneous values of the equilibrium constants. Therefore, we proceeded as follows.

For both mechanisms in Fig. 1 we wrote non-linear least-squares fitting routines which allowed the simultaneous fit of δ_{ba} and of δ_{cd} as a function of temperature, using either Eqns (1) and (2) in the case of the correlated transfer mechanism in Fig. 1(a) and Eqns (1), (6) and (7) in the case of the stepwise transfer mechanism in Fig. 1(b), by varying the intrinsic chemical shift difference Δ and the reaction entropies and enthalpies.

The parameters obtained for both mechanisms are given in Tables 2 and 3. The corresponding data fits are depicted in Figs 4(a) and Fig. 5(a), and both fits are satisfactory at low temperatures. The reaction entropies are very small and the reaction enthalpies are smaller than in solid porphyrins and tetraaza[14]annulenes.[3,4] Most remarkable is the intrinsic chemical shift difference of $\Delta = 46$ ppm in the case of the correlated transfer and $\Delta = 52$ ppm in the case of the stepwise transfer. These values represent roughly only half of the values found for porphyrin. This finding will be commented upon later. In Fig. 4(b) we compare the calculated values of log K_{12}^{A} and of log K_{12}^{B} as a function of the inverse temperature with the experimental values; in Fig. 5(b) are shown the corresponding graphs of log K_{ab} and log K_{dc} for the stepwise mechanism. The data fits are satisfactory in both cases. Figure 4(c) contains a population analysis for the correlated proton transfer and Figure 5(c) a similar analysis for the stepwise transfer. In all cases the states 1, assigned to a *trans*-tautomer, are the only states present below 50 K. In the correlated transfer first state 2 of molecule B and then state 2 of molecule A are populated. In the case of the stepwise transfer first the *cis*-tautomer 3 is populated whereas states 2 and 4 are quasi-degenerate and populated only above 200 K. Above 250 K all for states are populated almost to the same extent.

In both Figs 4(b) and 5(b) we observe that the theoretical curves do not describe well the experimental values derived from the chemical shift analysis in the region of room temperature. This discrepancy between the calculated and experimental values may indicate that a phase transition has occurred which renders the two molecules A and B at room temperature equivalent.

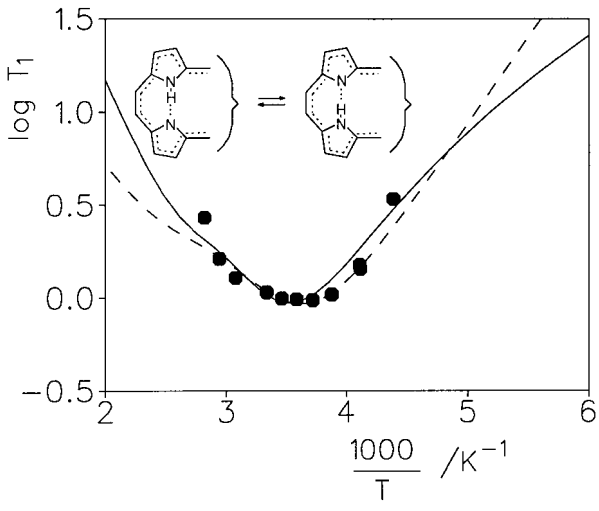

Figure 6. (a) Longitudinal ^{15}N relaxation times of porphycene obtained at a frequency of 9.12 MHz as a function of the inverse of temperature. The dashed line corresponds to an initial data fitting using the Arrhenius relation Eqn. (9) and the parameters of Eqn. (12). The solid line corresponds to the values calculated from the non-linear Arrhenius curve of the porphycene tautomerism shown in Fig. 7 as a solid line

^{15}N T_1 measurements

The longitudinal ^{15}N relaxation time measurements showed exponential magnetization decays and a single common relaxation time for the four ^{15}N signals at low temperatures. The T_1 values obtained by non-linear least-squares fitting are given in Table 4 and are plotted in Fig.

Table 5. Rate constants of polycrystalline porphycene calculated from ^{15}N T_1 relaxation

T(K)	$k(s^{-1})$	T(K)	$k(s^{-1})$
228	4.24×10^6	289	3.82×10^7
243	1.13×10^7	300	4.93×10^7
243.5	1.07×10^7	325	7.24×10^7
258	1.99×10^7	340	1.14×10^8
269	2.66×10^7	355	3.66×10^8
279	3.62×10^7		

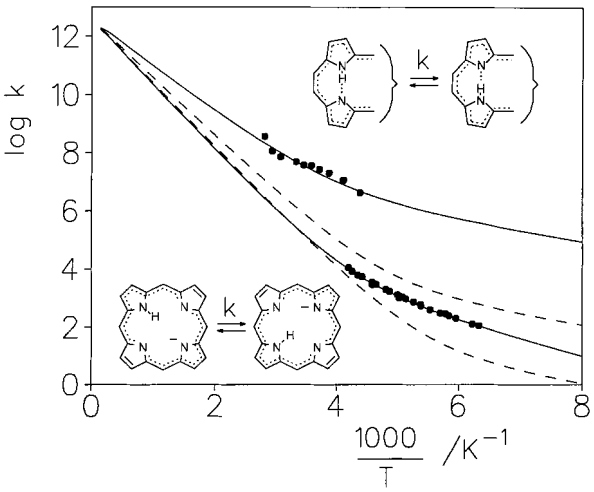

Figure 7. Arrhenius diagram of the proton motion in solid porphycene in comparison with the proton transfer in the porphyrin anion.[3f] The dashed lines refer to the predicted curves for the deuteron (upper line) and triton (lower line) transfer calculated as described previously using an additional barrier height of 7.74 kJ mol^{-1} for the deuteron and of 11.19 kJ mol^{-1} for the triton motion, and the tunneling masses 3.5 and 4.5

5(a) on a logarithmic scale as a function of the inverse of temperature. They exhibit the typical behavior of a thermally activated process. The observation of the minimum around 300 K allowed us to verify that the modulation of the heteronuclear dipolar ^{1}H–^{15}N interaction together with the fast proton motion is responsible for the longitudinal relaxation observed, as described in the following.

In principle, longitudinal relaxation in the presence of complex motions like the reaction network in Fig. 1(b) requires us to consider also complex spectral densities.[16] However, in the case of porphycene each single reaction step in Fig. 1 is quasi-degenerate according to the analysis in the preceding section. Therefore, we analyze the porphycene data in terms of a quasi-degenerate proton transfer mechanism, characterized by equal forward and backward rate constants $k_+ = k_- = k$, i.e. an equilibrium constant of $K \approx 1$, where either two protons are transferred in case of the correlated mechanism or one proton in the case of the stepwise mechanism.

As shown previously,[6] under MAS conditions the longitudinal relaxation times of the ^{15}N nuclei in a proton transfer system N—H···N ⇌ N···H—N is caused by the modulation of the ^{15}N –^{1}H dipolar interaction during the transfer process. The expression for T_1 is given by

$$\frac{1}{T_1} = \frac{1}{40}\gamma_N^2\gamma_H^2\left(\frac{h}{2\pi}\right)^2\left(\frac{\mu_0}{4\pi}\right)^2 D\left[\frac{4K}{(1+K)^2}\right]$$

$$\left[\frac{\tau_c}{1+(\omega_H-\omega_N)^2\tau_c^2}+\frac{3\tau_c}{1+\omega_N^2\tau_c^2}+\frac{6\tau_c}{1+(\omega_H+\omega_N)^2\tau_c^2}\right] \quad (8)$$

where τ_c is the correlation time of the proton motion whose temperature dependence may be expressed in a first approximation by the Arrhenius equation:

$$1/\tau_c = 2k = 2A\exp(-E_a/RT) \quad (9)$$

The factor D, representing the dipolar interaction, is given by[6]

$$D = r_1^{-6} + r_2^{-6} + r_1^{-3}r_2^{-3}(1 - 3\cos^2\alpha), \quad (10)$$

where α represents the angle between the NH vectors before and after the proton transfer, r_1 the short NH distance and r_2 the long NH distance across the hydrogen bond. A non-linear least-squares fitting program was written in order to calculate the solid line in Fig. 5(a) from which the parameters $E_a = 17.8 \pm 1.8$ kJ mol^{-1}, $A = 7 \pm 6$ 10^{10} s^{-1} and $D = 0.26 \pm 0.013$ Å^{-6} were obtained. The dashed line in Fig. 6 reproduces the experimental values in a satisfactory way around the T_1 minimum.

The Arrhenius approximation is valid only in a small temperature range because tunneling at low temperatures leads to non-linear Arrhenius curves.[11] Thus, using the above activation parameters we calculate a rate constant of $k \approx 250$ s^{-1} for a temperature of 110 K, which is not consistent with the experimental findings as this value should already induce a decoalescence of the ^{15}N signals. Therefore, it follows that the rate constant at 110 K must be larger because of tunneling. In order to obtain model-free rate constants we proceeded as follows. A computer program was written which allowed us to obtain the rate constant k of the tautomerism assumed to be quasi-

Table 6. Parameters of the modified Bell model of the tautomerism of porphyrin, the porphyrin anion and porphycene[a]

Species	E_d	E_m	$E_d + E_m$	Log A	$2a$	m_H	m_D	Δm
Porphyrin	28.7	22.7	51.4	12.6	0.68	1	2	1.5
Porphyrin anion	34.3	10.0	44.3	12.6	0.78	1	2	1.5
Porphycene, stepwise single H transfer	25.9	5.9	31.8	12.6	0.64	1	2	1.5
Porphycene, correlated HH transfer	25.9	5.9	31.8	12.6	0.56	2	4	1.5

[a] Barrier height E_d and minimum energy for tunneling E_m in kJ mol^{-1}, barrier width $2a$ in Å, frequency factor A in s^{-1}. Tunneling masses $m_{eff}^{L} = m_L + \Delta m$, L = H, D.

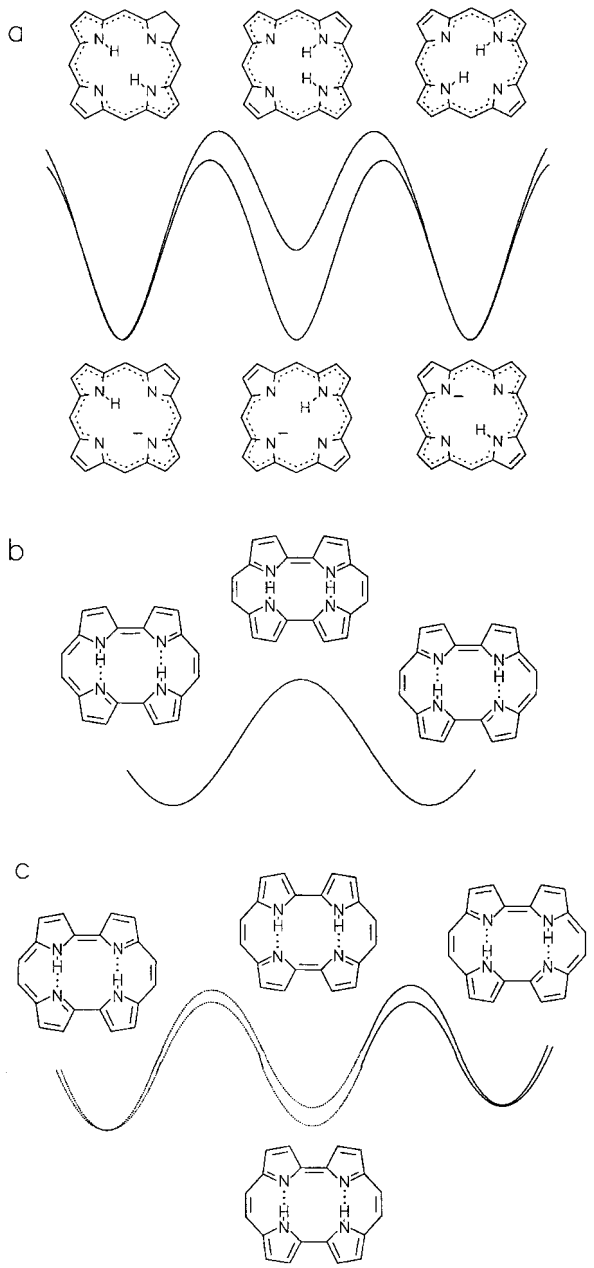

Figure 8. Reaction energy profiles (schematic) for (a) the tautomerism of porphyrin and the porphyrin anion, (b) the correlated double proton transfer and (c) the stepwise proton transfer mechanism in polycrystalline porphycene

degenerate with the ^{15}N relaxation time T_1 and the factor D as input, which was assumed to be independent of temperature. The values obtained are listed in Table 5 and plotted in Figure 7 in a logarithmic manner as a function of the inverse of temperature. For comparison, we also plotted the values of the tautomerism of the porphyrin anion reported previously.[3f] and all important experimental parameters are given in Table 6.

The solid lines were calculated in terms of a modified Bell tunneling model as described in Ref. 3f The parameters used are included in Table 7. The parameter sets listed are not definite and may change if further rate constants would be included. The data could be equally well be fitted in terms of the correlated double proton transfer and the stepwise transfer. In a last stage, the calculated rate constants of the porphycene tautomerism shown in Fig. 7 were converted into ^{15}N T_1 values depicted in Fig. 6 as a solid line. The data fit is more satisfactory than the simple Arrhenius fit.

DISCUSSION

Using ^{15}N solid-state NMR we have been able to characterize the tautomerism of porphycene established previously[3b] with respect to (i) the thermodynamics by analyzing the temperature-dependent signal positions and (ii) with respect to the kinetics and the proton locations by analyzing the ^{15}N longitudinal relaxation times. From the latter information about the hydrogen bond geometries, in particular the proton locations, is also obtained. The results are discussed below.

Thermodynamics of porphycene proton tautomerism

The analysis of the ^{15}N chemical shifts of porphycene was presented in Fig. 4 for the correlated and in Fig. 5 for the stepwise reaction mechanism in Fig. 1. The intrinsic chemical shift difference Δ between the protonated and non-protonated nitrogen atoms was assumed to be independent of temperature. Both mechanisms can explain the experimental data. The agreement is good at low temperatures but less satisfactory around room temperature. Therefore, we have the suspicion that at 300 K a phase transition has occurred in which the protons are truely disordered, as indicated by the room-temperature crystal structure. In terms of the correlated double proton transfer mechanism this would mean that the difference between molecules A and B has disappeared, as indicated by the crystal structure analysis.[7] In terms of the stepwise mechanism this would mean that all four tautomeric states exhibit the same probability; in other words, each proton alone would move in a symmetric potential well, where decoupling with the motion of the other proton has occurred. This result is, however, not very plausible. In conclusion, by the chemical shift analysis alone it cannot be decided whether the proton motion is correlated or stepwise, but the correlated transfer seems to be more realistic. Therefore, the validity of the thermodynamic parameters obtained still depend on the interpretation of the reaction mechanism. Therefore, a discussion of margins of errors of the measurements is not appropriate at present.

Table 7. Summary of kinetic results of the proton transfer in porphyrin, the porphyrin anion and porphycene[a]

Species	$\mathrm{Log}A^{\mathrm{obs}}$	$E_a{}^{\mathrm{obs}}$	T_{min}	T_{max}	k(298 K)
Porphyrin	10.7	37.2	209	290	15600
Porphyrin anion	7.8	17.7	158	238	10^5
Porphycene	10.8	17.8	228	355	5×10^7

[a] Frequency factors A^{obs} in s^{-1}, activation energies $E_a{}^{\mathrm{obs}}$ observed at 298 K in kJ mol^{-1}, k (rate constants of single proton transfer) in s^{-1}, T_{min}, T_{max} (temperature range where rate constants were determined) in K.

Kinetics of porphycene proton tautomerism

As each reaction mechanism implies a near-degenerate single or double proton motion, the analysis of the longitudinal relaxation times was therefore based on the assumption of a simplified quasi-degenerate incoherent proton transfer as indicated in Figs 7 and 8. This means that we neglect in the case of a correlated transfer the difference between molecules A and B in the unit cell with respect to the proton transfer dynamics. In the single proton transfer case the rate constants derived would correspond to the single steps in Fig. 1(b), which are each assumed to be quasi-degenerate.

Table 6 indicates that the experimental pre-exponential factors A^{obs} of the Arrhenius curves are much smaller than the true pre-exponential factor of about $10^{12.6}$ s^{-1} (Table 7) expected for intramolecular reactions because of tunneling contributions at low temperatures. The slope of the non-linear Arrhenius curves at very low temperatures is interpreted in terms of a minimum energy E_{m} for tunneling to occur which is assumed to be of the same order for both porphycene and the porphyrin anion. This value may not have a real physical meaning but was found to be necessary to be introducted into the Bell model as the Arrhenius curves could not be reproduced otherwise. E_{m} could be some measure of a heavy atom rearrangement of the molecular backbones associated with the compression of the internal hydrogen bonds, a process which assists the proton transfer. The slope at very high temperatures is given by $E_{\mathrm{m}} + E_{\mathrm{d}}$, which may be regarded as the effective barrier. This barrier is substantially smaller in the case of porphycene (Table 7) as compared with the porphyrin anion, but larger than the effective energies of activation. This finding and the smaller barrier width $2a$ is consistent with the stronger hydrogen bonds in porphycene. The tunneling masses used were similar to those in the porphyrin anion case where we had to add an additional mass arising from some heavy atom tunneling.[3f] The predicted Arrhenius curves for the deuteron and triton transfer in porphycene are included as dashed lines in Fig. 7. The calculated Arrhenius curves are subject to a large margin of systematic errors. However, they may stimulate to perform further dynamic NMR experiments on the deuterated and the tritiated systems as the rate constants of these isotopologs are predicted for the micro- to millisecond time-scale where they should be measurable by lineshape analysis.

The energy profile of the tautomerism of porphyrin, the porphyrin anion, the correlated double and the stepwise single proton transfer in porphycene resulting from the interpretation of our experiments is depicted in Fig. 8. First, we note that the tautomeric processes in porphyrins,[3d,e] tetraaza[14]annulenes,[4] azophenine[8] and oxalamidine[17] were found to be stepwise. Thus, at first sight one might argue that a stepwise reaction mechanism should be also realized in the porphycene case. However, so far neither other spectroscopic experiments in addition to those presented previously[3b] and in this paper nor theoretical calculations have been able to identify *cis*-tautomers of porphycene.[9]

Hydrogen bond geometry and ^{15}N chemical shifts

More information concerning the process detected comes from the interpretation of the geometric factor D in Eqn. (8) whose value for porphycene 0.26 ± 0.013 $Å^{-6}$ as given earlier. From this value we obtain in fact information about the porphycene hydrogen bond geometry. As the crystallographic NN bond distance of porphycene, $r_{\mathrm{NN}} = 2.63$ Å,[7] is well known in contrast to the proton locations, we obtain by simple arithmetic the following relation involving the short and the long NH distances r_1 and r_2 of the porphycene hydrogen bonds, i.e.

$$\arccos\left[\sqrt{\frac{1}{3}(1 - r_1^3 r_2^3 (D - r_1^6 - r_2^6))}\right] \qquad (11)$$

$$= \arccos\left[\sqrt{\frac{r_1^2 - r_2^2 + r_{\mathrm{NN}}^2}{2r\mathrm{NN}r_1}}\right] - \arccos\left[\sqrt{\frac{-r_1^2 + r_2^2 + r_{\mathrm{NN}}^2}{2r\mathrm{NN}r_2}}\right]$$

In this equation we neglect the fact that the distances obtained by NMR taking advantage of the dipolar coupling represent the cubic average distances and not the mean average distances. Equation (11) is not yet sufficient to determine the two NH distances r_1 and r_2 and the hydrogen bond angle NHN. In order to obtain these parameters we make use of the universal hydrogen bond

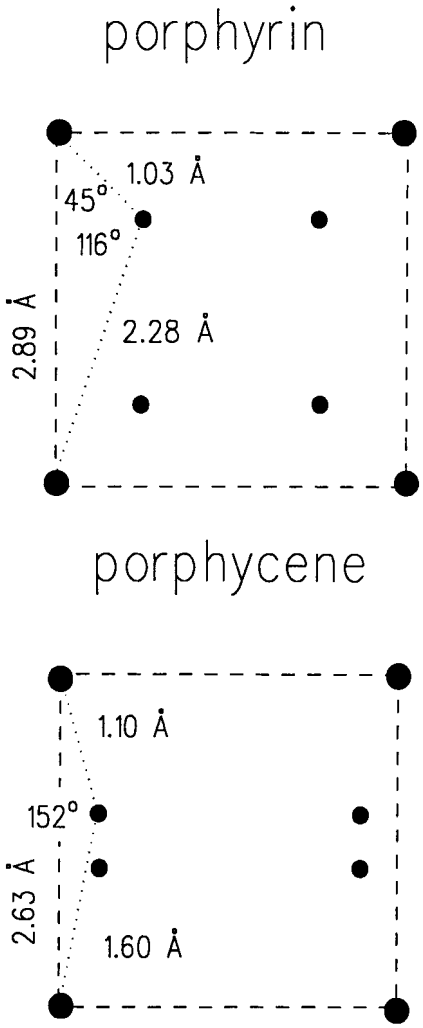

Figure 9. Hydrogen bond geometries of porphyrin and porphycene. The geometry of porphyrin was calculated using the hydrogen bond correlation of Eqn. (12) and assuming an angle of 45° between the NH and the NN vectors. The geometry of porphycene was calculated from the relaxation data given in the text and the hydrogen bond correlation Eqn. (11)

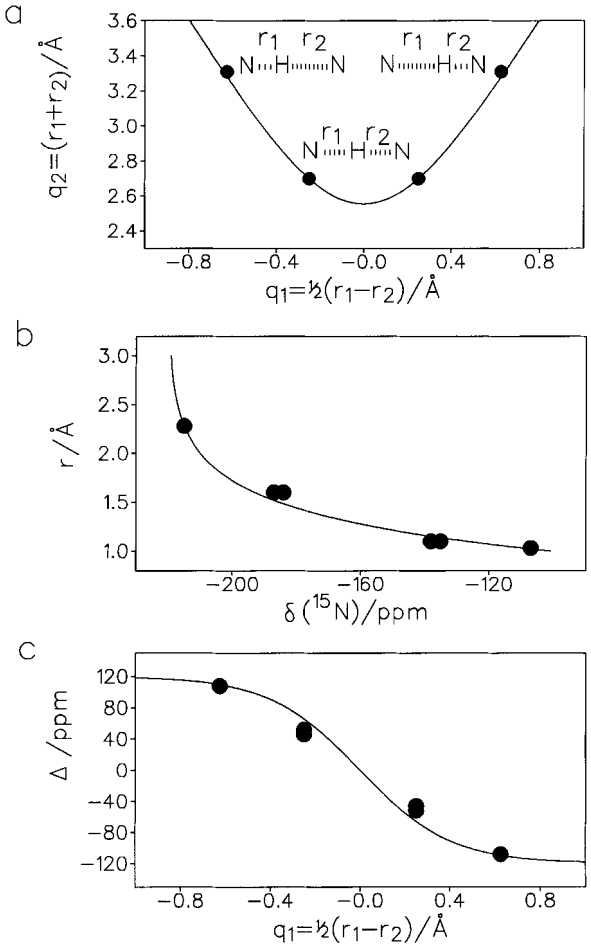

Figure 10. (a) Hydrogen bond correlation for porphyrin and porphycene. r_1 and r_2 represent the two N···H distances of the corresponding N—H···N hydrogen bonds, $q_1 = \frac{1}{2}(r_1 - r_2)$ the proton transfer coordinate and $q_2 = r_1 + r_2$ the heavy atom coordinates. The solid line was calculated according to Eqn. (13). (b) Dependence of the ^{15}N chemical shifts of porphyrin and porphycene as a function of the N···H distance. The solid line was calculated according to Eqn. (14). (c) Intrinsic chemical shift difference of the two ^{15}N nuclei of the N—H···N units of porphyrin and porphycene as a function of q_1. The solid line was calculated according to Eqns (11) and (14)

correlation for NHN hydrogen bonds arising from neutron diffraction data[18] and NMR and theoretical data,[19] i.e.

$$r_2 = r_0 - b\ln\{1 - \exp[-(r_1 - r_0)/b]\} \qquad (12)$$

with $b = 0.404$ Å and $r_0 = 0.99$ Å. This equation is valid not only for linear but also for non-linear hydrogen-bonded systems. Now, Eqns (11) and (12) provide two independent expressions from which the values $r_1 = 1.10$ Å and $r_2 = 1.60$ Å were calculated by substituting Eqn. (12) into Eqn. (11) and numerical solution of the resulting equation. These values imply a hydrogen bond angle of 152° (Fig. 9). To our knowledge, these results are the first (experimental and theoretical) which give an estimation of the proton locations in porphycene.

For the porphyrin molecule the NHN geometry was estimated as follows. We assume an angle of 45° between the short NH vector and the NN vector (Fig. 9). Furthermore, we take into account the crystallographic NN distance of 2.89 Å.[20] Next we modify the above hydrogen bond correlation for the presence of a bifurcated very weak hydrogen bond of the inner proton to the adjacent two non-protonated nitrogen atoms, i.e. we write

$$r_2 = r_0 - b\ln(0.5\{1 - \exp[-(r_1 - r_0)/b)\}) \qquad (13)$$

with $b = 0.404$ Å and $r_0 = 0.997$ Å. We obtain the parameters $r_1 = 1.03$ Å, $r_2 = 2.28$ Å and a hydrogen bond

angle of 116°. The short NH distance is almost identical with the distance of 1.02 Å found in previous NMR relaxation time measurements[20] for *meso*-tetraphenylporphyrin dissolved in toluene,[21] which confirms the NHN-hydrogen bond correlation for porphyrins.

Figure 9 indicates that the protons in porphyrin and its anion have to jump across a large distance of more than 1 Å. By contrast, the proton transfer distances in porphycene are much smaller, i.e. around half of the porphyrin value, because of the strong hydrogen bonds. The latter are stronger than in porphyrin not only because of the somewhat shorter NN distance but especially because of the larger hydrogen bond angle allowed by the molecular backbone.

By rearranging Eqn. (11) it follows that the sum $q_2 = r_1 + r_2$ is a function of the proton transfer coordinate $q_1 = {}^{1/2}(r_1 - r_2)$,[19] i.e.

$$q_2 = 2r_0 + 2q_1 + 2b\ln[1 + \exp(-2q_1/b)] \qquad (14)$$

with $b = 0.404$ Å and $r_0 = 0.997$ Å. In Fig. 10(a) we have plotted q_2 as a function of q_1 as a solid line, together with the values (filled circles) for porphyrin and porphycene. Each pair of circles at a given value of q_2 indicates the two quasi-degenerate tautomeric states between which the proton transfers occur. The correlation line is a crude guideline of the two-dimensional minimum reaction energy pathway. This pathway will consist of a combination of a hydrogen bond compression, i.e. the motion along the correlation line and actual proton transfers at a constant reduced q_2 value. It is clear from Fig. 10(a) that the barrier of proton transfer will be smaller in the porphycene case as the barrier will vanish for a hypothetical system where the proton is located in the hydrogen bond center. However, there is no simple relation between the molecular geometry and the barrier of proton transfer as the energy to compress the hydrogen bond during the proton transfer plays a major role, which will depend on the rigidity of the molecular backbone rather than on the molecular geometry.

The above treatment bears the simplification that only one set of coordinates q_2 and q_1 is considered, which is valid in the case of a single proton transfer or in the case of a concerted double proton transfer. The latter case would naturally be realized if the compression of one hydrogen bond also leads to a compression of the second bond. However, in this study it was not possible to determine the cooperativity of both hydrogen bonds, which will be a challenging task for the future.

We note that the chemical shift analysis in Figs 4(a) and 5(a) provides further insight into the hydrogen bond properties of porphycene. Using the average high-temperature chemical shift of 161 ppm and the intrinsic chemical shift differences of $\Delta = 46$ ppm for the correlated double proton transfer ($\Delta = 52$ ppm for the stepwise transfer), we obtain chemical shifts of 135 and 187 ppm (138 and 184 ppm) for the NH and the —N= nuclei, whereas these values were 107 and 215 for porphyrin.[3b] In Fig. 10(b) we have plotted the data as a function of the N···H distance. The data were fitted to the simple equation whose form was proposed previously:[22]

$$\delta({}^{15}\mathrm{N}) = 220 - 120\exp[-(r_1 - r_0)/b] \qquad (15)$$

where the fit parameters were adapted to the experimental data of Fig. 10(b) by a non-linear least-squares fit, depicted as a solid line. We note that Eqn. (15) is preliminary, but may serve as a reference in the future in order to establish general relations between ^{15}N chemical shifts and NH distances in porphyrinoids. Finally, in Fig. 10(c) we have plotted the intrinsic chemical shift difference Δ between the two types of porphycene nitrogen atoms as a function of the proton transfer coordinate. The solid line was calculated from Eqns (12) and (14). It is seen that Δ is a measure of the proton transfer distances.

Finally, we note an interesting observation of Galiersley *et al.*[9b] on the optical spectra of porphycene in a rare gas matrix. They found evidence for a coherent tunnel process in the electronic excited state and the ground state. As coherent tunneling requires a degeneracy of the initial and the final states, the process was attributed to a direct interconversion between the two *trans*-tautomers of porphycene. These findings are not at all in contrast to our results concerning polycrystalline porphycene, where the degeneracy between the states is broken by the crystal field, thus, rendering the proton transfer incoherent. The barrier parameters reported here may, however, be useful in the future for calculating the tunnel frequencies manifest in the optical spectra.

CONCLUSIONS

Using ^{15}N solid-state NMR we studied the thermodynamics and the dynamics of proton transfer in polycrystalline porphycene, where rate constants of the incoherent process were obtained on the nanosecond time-scale by analysis of the longitudinal ^{15}N relaxation times. The analysis also provided information about the hydrogen bond geometries of porphycene, in comparison with porphyrin. The analysis of the dependence of the rate constants on temperature revealed a barrier height of about 32 kJ mol^{-1}, which is much lower than that for the porphyrin anion. This result is rationalized in terms of the shorter hydrogen bonds in porphycene. The barrier obtained may serve as a guideline for comparison with values calculated by *ab initio* methods in the future. We predict major kinetic H/D/T isotope effects on the micro- to millisecond time-scale which may be measured in the future using NMR lineshape analysis. The detailed nature of the proton transfer process observed could not be revealed; it corresponds either to quasi-degenerate

stepwise single proton transfer with two decoupled intramolecular hydrogen bonds or to a correlated quasi-degenerate double proton transfer with a strong coupling between the two hydrogen bonds. As the latter is more plausible, we think that the correlated transfer is the more probable mechanism. Finally, we have shown that the hydrogen bond correlation theorem is useful for predicting the geometries of non-linear intramolecular hydrogen bonds in heterocyclic compounds.

Acknowledgements

The financial support of the Deutsche Forschungsgemeinschaft, Bonn-Bad Godesberg, and the Fonds der Chemischen Industrie, Frankfurt, is gratefully acknowledged.

REFERENCES

1. Elguero J, Marzin C, Katrizky AR, Linda P. *The Tautomerism of Heterocycles*. Academic Press: New York, 1976 (the 2nd edition of this book will appear in 2000).
2. (a) Baldy A, Elguero J, Faure R, Pierrot M, Vincent EJ. *J. Am. Chem. Soc.* 1985; **107**: 5290; (b) Smith JAS, Wehrle B, Aguilar-Parrilla F, Limbach HH, Foces-Foces MC, Cano FH, Elguero J, Baldy A, Pierrot M, Khurshid MMT, Larcombe-McDouall JB. *J. Am. Chem. Soc.* 1989; **111**, 7304; (c) Aguillar-Parrilla F, Limbach HH, Blanz M, Rayner TJ, Smith JAS. *Magn. Reson. Relat. Phenom.* 1990; **25**, 615; (d) Aguilar-Parrilla F, Cativiela C, Diaz de Villegas MD, Elguero J, Foces-Foces MC, Laureiro JIG, Cano FH, Limbach HH, Smith JAS, Toiron C. *J. Chem. Soc., Perkin Trans. 2* 1992; 1737; (f) Aguilar-Parrilla F, Scherer G, Limbach HH, Foces-Foces MC, Cano FH, Smith JAS, Toiron C, Elguero J. *J. Am. Chem. Soc.* 1992; **114**, 9657; (g) Toda F, Tanaka K, Foces-Foces MC, Llamas-Saiz AL, Limbach HH, Aguilar-Parrilla F, Claramunt RM, Lopez C, Elguero J. *J. Chem. Soc., Chem. Commun.* 1993; 1139; (h) Aguilar-Parrilla F, Claramunt RM, Lopez C, Sanz D, Limbach HH, Elguero J. *J. Phys. Chem.* 1994; **98**, 8752; (i) Elguero J, Cano FH, Foces-Foces MC, Llamas-Saiz AL, Limbach HH, Aguilar-Parrilla F, Claramunt RM, Lopez C. *J. Heterocycl. Chem.* 1994; **31**, 695; (j) Aguilar-Parrilla F, Männle F, Limbach HH, Elguero J, Jagerovic N. *Magn. Reson. Chem.* 1994; **32**, 699; (k) Lamas-Saiz AL, Foces-Foces MC, Cano FH, Elguero J, Jimenez P, Laynez J, Meutermans W, Elguero J, Limbach HH, Aguilar-Parrilla F. *Acta Crystallogr., Sect. B* 1994; **50**, 746; (l) Aguilar-Parrilla F, Limbach HH, Foces-Foces MC, Cano FH, Jagerovic N, Elguero J. *J. Org. Chem.* 1995; **60**, 1965; (m) Elguero J, Jagerovic N, Foces-Foces MC, Cano FH, Roux MV, Aguilar-Parrilla F, Limbach HH. *J. Heterocycl. Chem.* 1995; **32**, 451; (n) Hoelger CG, Limbach HH, Aguilar-Parrilla F, Elguéro J, Weintraub O, Vega S. *J. Magn. Reson. A* 1996; **120**, 46; (o) Lopez C, Claramunt RM, Llamas-Saiz A, Foces-Foces MC, Elguero J, Sobrados I, Aguilar-Parrilla F, Limbach HH. *New J. Chem.* 1996; **20**, 523; (p) de Paz JLG, Elguero J, Foces-Foces MC, Llamas-Saiz A, Aguilar-Parrilla F, Klein O, Limbach HH. *J. Chem. Soc., Perkin Trans. 2* 1997; 101; (q) Aguilar-Parrilla F, Klein O, Elguero J, Limbach HH. *Ber. Bunsenges. Phys. Chem.* 1997; **101**, 884; (r) Anulewicz R, Wawer I, Krygowski TM, Männle F, Limbach H-H. *J. Am. Chem. Soc.* 1997; **119**, 12223; (s) Männle F, Wawer I, Limbach HH. *Chem. Phys. Lett.* 1996; **256**, 657.
3. (a) Limbach HH, Hennig J, Kendrick RD, Yannoni CS. *J. Am. Chem. Soc.* 1984; **106**: 4059; (b) Wehrle B, Limbach HH, Köcher M, Ermer O, Vogel E. *Angew. Chem.*, 1987; **99**: 914; *Angew. Chem., Int. Ed. Engl.* 1987; **26**: 934; (c) Wehrle B, Limbach HH. *Chem. Phys.* 1989; **136**: 223; (d) Braun J, Schlabach M, Wehrle B, Köcher M, Vogel E and Limbach HH. *J. Am. Chem. Soc.* 1994; **116**: 6593; (e) Braun J, Limbach HH, Williams P, Morimoto H, Wemmer D. *J. Am. Chem. Soc.* 1996; **30**: 7231; (f) Braun J, Schwesinger R, Williams PG, Morimoto H, Wemmer DE, Limbach HH. *J. Am. Chem. Soc.* 1996; **118**: 11101; (g) Frydman B, Fernandez CO, Vogel E. *J. Org. Chem.* 1998; **63**: 9835.
4. (a) Limbach HH, Wehrle B, Zimmermann H, Kendrick R, Yannoni CS. *Angew. Chem.* 1987; **99**: 241; *Angew. Chem., Int. Ed. Engl.* 1987; **26**: 247; (b) Limbach HH, Wehrle B, Zimmermann H, Kendrick R, Yannoni CS. *J. Am. Chem. Soc.* 1987; **109**: 929; (c) Wehrle B, Zimmermann H, Limbach HH. *J. Am. Chem. Soc.* 1988; **110**: 7014; (d) Wehrle B, Aguilar-Parrilla F, Limbach HH. *J. Magn. Reson.* 1990; **87**: 584; (e) Aguilar-Parrilla F, Wehrle B, Bräunling H, Limbach HH. *J. Magn. Reson.* 1990; **87**: 592; (f) Benedict C, Langer U, Limbach HH, Ogata H, Takeda S. *Ber. Bunsenges. Phys. Chem.* 1998; **102**: 335.
5. Limbach HH, Wehrle B, Schlabach M, Kendrick R, Yannoni CS. *J. Magn. Reson.*, 1988; **77**: 84.
6. Hoelger CG, Wehrle B, Benedict H, Limbach HH. *J. Phys. Chem.* 1994; **98**: 843.
7. Vogel E, Köcher M, Schmickler H, Lex J. *Angew. Chem.* 1986; **98**: 262; *Angew. Chem., Int. Ed. Engl.* 1986; **26**: 257.
8. Rumpel H, Limbach HH. *J. Am. Chem. Soc.*, 1989; **111**: 5429.
9. (a) Malsch K, Hohlneicher G. *J. Phys. Chem. A* 1997; **101**: 8409; (b) Galievsky V, Starukhin A, Vogel E, Waluk J. *J. Phys. Chem. A* 1998; **102**: 4966.
10. Starukhin A, Vogel E, Waluk J. *J. Phys. Chem. A* 1998; **102**: 9999.
11. Bell RP. *The Tunnel Effect*, Chapman and Hall, London 1980.
12. Torchia DAJ. *Magn. Reson.* **30**: 613 (1978).
13. Du Bois Murphy P. *J. Magn. Reson.*, 1986; **70**: 307.
14. Some authors[15] use neat nitromethane for ^{15}N CP MAS chemical shifts but although these shifts can be converted into solid $^{15}NH_4Cl$ reference by using δ $CH_3NO_2 + 338.1$ ppm (355.3 ppm from CH_3NO_2 to saturated $^{15}NH_4Cl$–D_2O and -17.2 ppm from saturated $^{15}NH_4Cl$–D_2O to solid $^{15}NH_4Cl$),[15] they are not directly comparable because they have been calculated by using some approximate relationship between chemical shift references.[15]
15. (a) Witanowski M, Stefaniak L, Szymanski S, Januszewski H. *J. Magn. Reson.* 1977; **28**: 217; (b) Witanowski M, Stefaniak L, Webb GA. *Annu. Rep. NMR Spectrosc.* 1981; **11B**; (c) Martin G, Martin ML, Gouesnard JP. *NMR— Basic Principles and Progress*, vol. 18. Springer: Heidelberg, 1989; (d) Srinivasan PR, Lichter RL. *J. Magn. Reson.* 1977; **28**: 227.
16. (a) Andrew ER, Latanowicz L. *J. Magn. Reson.* 1986; **68**: 232; (b) Latanowicz L, Reynhardt EC. *Ber. Bunsenges. Phys. Chem.* 1994; **98**: 818; (c) Latanowicz L, Reynhardt EC, Utrecht R, Medycki W. *Ber. Bunsenges. Phys. Chem.* 1995; **99**: 152; (d) Reynhardt EC, Latanowicz L. *Chem. Phys. Lett.*, 1996; **251**: 235; (e) Takeda S, Inabe T, Benedict C, Langer U, Limbach HH. *Ber. Bunsenges. Phys. Chem.* 1998; **102**: 1358.
17. (a) Scherer G, Limbach HH. *J. Am. Chem. Soc.* 1989; **111**: 5946; (b) Scherer G, Limbach HH. *J. Am. Chem. Soc.* 1994; **116**: 1230; (c) Scherer G, Limbach HH. *Croat. Chem. Acta* 1994; **67**: 431.
18. (a) Steiner Th, W. Saenger W. *Acta Crystallogr., Sect. B* 1994; **50**: 348; (b) Steiner Th. *J. Chem. Soc., Chem. Commun.* 1995; 1331; (c) Gilli P, Bertolasi V, Ferretti V, Gilli G. *J. Am. Chem. Soc.* 1994; **116**: 909.
19. Benedict H, Limbach HH, Wehlan M, Fehlhammer WP, Golubev NS, Janoschek R. *J. Am. Chem. Soc.* 1998; **120**: 2939.
20. (a) Webb LE, Fleischer EB. *J. Chem. Phys.* 1965; **43**: 3100; (b) Chen BML, Tulinsky A. *J. Am. Chem. Soc.* 1972; **94**: 4144; (c) Hennig J, Limbach HH. *J. Am. Chem. Soc.*, 1984; **106**: 292.
21. Hennig J, Limbach HH. *J. Am. Chem. Soc.* 1984; **106**: 292.
22. Smirnov SN, Benedict H, Golubev NS, Denisov GS, Kreevoy MM, Schowen RL, Limbach HH. *Can J. Chem.* 1999; **77**: 943.

